

Radiolabeled methotrexate as a diagnostic agent of inflammatory target sites: A proof-of-concept study

MARIA PAPACHRISTOU^{1*}, GEORGE A. KASTIS^{2,3*}, PETROS Z. STAVROU¹, STAVROS XANTHOPOULOS³, LARS R. FURENLID^{4,5}, IOANNIS E. DATSERIS¹ and PENELOPE BOUZIOTIS^{3*}

¹Department of Nuclear Medicine-PET/CT, General Hospital of Athens 'Evangelismos', 10676 Athens;

²Research Center of Mathematics, Academy of Athens, 11527 Athens; ³Institute for Nuclear and Radiological Sciences and Technology, Energy and Safety, National Center for Scientific Research 'Demokritos', 15310 Athens, Greece;

⁴Center for Gamma-Ray Imaging, Department of Medical Imaging, University of Arizona, Tucson, AZ 85724;

⁵College of Optical Sciences, University of Arizona, Tucson, AZ 85721, USA

Received July 11, 2017; Accepted November 7, 2017

DOI: 10.3892/mmr.2017.8166

Abstract. Methotrexate (MTX), as a pharmaceutical, is frequently used in tumor chemotherapy and is also a part of the established treatment of a number of autoimmune inflammatory disorders. Radiolabeled MTX has been studied as a tumor-diagnostic agent in a number of published studies. In the present study, the potential use of technetium-99m-labelled MTX (^{99m}Tc-MTX) as a radiotracer was investigated for the identification of inflammatory target sites. The labeling of MTX was carried out via a ^{99m}Tc-gluconate precursor. Evaluation studies included *in vitro* stability, plasma protein binding assessment, partition-coefficient estimation, *in vivo* scintigraphic imaging and *ex vivo* animal experiments in an animal inflammation model. MTX was successfully labelled with ^{99m}Tc, with a radiochemical purity of >95%. Stability was assessed in plasma, where it remained intact up to 85% at 4 h post-incubation, while protein binding of the radiotracer was observed to be ~50% at 4 h. These preclinical *ex vivo* and *in vivo* studies indicated that ^{99m}Tc-MTX accumulates in inflamed tissue, as well as in the spinal cord, joints and bones; all areas with relatively high remodeling activity. The results are promising, and set the stage for further work on the development and application of ^{99m}Tc-MTX as a radiotracer for inflammation associated with rheumatoid arthritis.

Introduction

Methotrexate {MTX; (2S)-2-[[4-[(2,4-diaminopteridin-6-yl)methyl-methylamino]benzoyl]amino]pentanedioic acid} is a structural analogue of folic acid and one of the most widely used antimetabolites in cancer chemotherapy (1). At low doses (up to 25 mg/week) it is also part of the established treatment of many autoimmune inflammatory disorders, most notable of which is rheumatoid arthritis (RA) where it has nowadays become the standard of care (2).

Folic acid is essential for the synthesis of deoxyribonucleic acids (DNA), since it is a required co-factor for the synthesis of thymidylate by the enzyme thymidylate synthetase (TS), but also plays a key role in purine metabolism, being a co-factor for the enzyme 5-aminoimidazole-4-carboxamide ribonucleotide (AICAR) transformylase. In order to be used as co-factor, folate needs to be converted to its active form by a two-step reaction that reduces folate first to dihydrofolate and subsequently to tetrahydrofolate (FH4). This last reaction is catalysed by the enzyme dihydrofolate reductase (DHFR) (3,4).

MTX inhibits DHFR, thus, it inhibits both TS and AICAR transformylase. In this way, MTX interferes with DNA synthesis, repair, and cellular replication, ultimately causing limitation of the high turnover of inflammatory cells. On the other hand, MTX-polyglutamates (MTX-glu) are long-lived metabolites of MTX, which reside in a variety of tissues, such as liver, erythrocytes and adipose tissue. They persist for weeks to months, and this is considered to be the key factor behind the slow onset and prolonged duration of the anti-inflammatory effects of MTX. In fact, it takes about a week for the onset of the anti-inflammatory effects, while MTX is almost undetectable 24 h after administration (3).

MTX-glu causes accumulation of AICAR, due to the AICAR transformylase inhibition, and its metabolites, which are inhibitors of adenosine deaminase and AMP deaminase, ultimately leading to elevated levels of both intracellular and extracellular adenosine. When MTX is administered at low doses, it induces elevated levels of extracellular adenosine, which mainly binds to A2 receptors and leads to increased intracellular cAMP, thus, leading to immunosuppression via

Correspondence to: Dr Maria Papachristou, Department of Nuclear Medicine-PET/CT, General Hospital of Athens 'Evangelismos', 45-47 Ypsilantou, 10676 Athens, Greece
E-mail: papacmaria@yahoo.gr

*Contributed equally

Abbreviations: MTX, methotrexate; RA, rheumatoid arthritis

Key words: radiolabeling, technetium-99m, methotrexate, rheumatoid arthritis, inflammation, imaging, hydroxyapatite

inhibition of phagocytosis, lymphocyte proliferation and of the secretion of various cytokines (4,5).

Other proposed actions of MTX in the treatment of RA include reduction of various cell adhesion molecules' expression, indirect inhibition of osteoclast formation and probably some indirect anti-angiogenic effects (6).

MTX has been studied as a tumor-diagnostic agent in a number of published studies, by either direct labelling with technetium-99m (^{99m}Tc) (7-9) or as a mercaptoacetyltriglycine-MTX (MAG3-MTX) conjugate labelled with ^{99m}Tc (10). The purpose of this study is to present the possible use of ^{99m}Tc -labelled MTX as a radiotracer for the identification of inflammatory target sites, which are associated with RA in joints, bones and tissues.

Materials and methods

All chemicals employed for this research were of analytical grade. Stannous chloride, ascorbic acid and sodium bicarbonate were purchased from Aldrich, USA. The ^{99m}Tc -generator was purchased from GE Healthcare. MTX was purchased from Pfizer (Athens, Greece). Saline and water for injection were purchased from Demo (Athens, Greece).

High-performance liquid chromatography (HPLC) analyses were performed on a Waters μ -Bondapak C18 (3.9 mm i.d. x300 mm) cartridge column (Waters GmbH, Eschborn, Germany). The gradient system employed is described below. Solvents for HPLC were of analytical grade, and were filtered through 0.22 μm membrane filters (EMD Millipore, Billerica, MA, USA) and degassed. Radioactivity measurements were recorded on an automated well-type γ -counter NaI(Tl) crystal (Packard).

Animal experiments were carried out according to European and National regulations. Biodistribution studies were performed using female normal Swiss mice (20 \pm 2 g) of the same colony and age, purchased from the Breeding Facilities of the Institute of Biosciences and Applications, NCSR 'Demokritos'.

Radiolabeling and radiochemical purity analysis. The labelling of MTX was performed by ligand exchange from a $^{99m}\text{Tc}(\text{v})\text{O}$ -gluconate precursor. Sodium gluconate acts as an intermediate exchange ligand for ^{99m}Tc , with stannous chloride as the reducing agent (11). Briefly, a solid mixture of 1 g sodium gluconate, 2 g of sodium bicarbonate and 15 mg of stannous chloride was homogenized and kept under anhydrous conditions. 3 mg of this mixture were dissolved in 1 ml of a sodium pertechnetate solution ($\text{Na}^{99m}\text{TcO}_4$) containing 296 MBq/8 mCi ^{99m}Tc . 10 mg of MTX were added, and the mixture was stirred for 30 min at room temperature. The pH of the final solution was 7.

Radiochemical control of the ^{99m}Tc -MTX complex was carried out with Instant Thin Layer Chromatography-Silica Gel (ITLC-SG) in saline and Whatman 3 mm chromatography paper (PC) in acetone. Briefly, 2 μl of the reaction mixture were applied on Silica Gel (ITLC-SG) and Whatman 3-mm strips. The radiochromatographs were developed in saline (0.9% NaCl) and acetone, respectively, over a distance of 10 cm. After drying, the strips were cut in 1-cm pieces and their radioactivity was counted in a well-type scintillation counter. Furthermore,

Reversed-Phase HPLC (RP-HPLC) analysis was performed on an aliquot of the reaction solution, by applying the following linear gradient system: From 0 to 80% solvent B (1-20 min), 80% solvent B (20-23 min), 80 to 0% solvent B (23-25 min) and 0% solvent B (25-30 min), at a 0.8 ml/min flow rate (solvent A: 0.1% Trifluoroacetic Acid (TFA) in H_2O ; solvent B: 0.1% TFA in Acetonitrile (AcCN)).

In vitro stability and protein binding. *In vitro* stability of ^{99m}Tc -MTX at room temperature was assessed up to 24 h after preparation of the sample. Plasma stability was carried out in fresh human plasma at 37°C. For preparation of human plasma, a blood sample from healthy donors was collected in heparinised polypropylene tubes and was immediately centrifuged at 2,000 x g for 10 min. The supernatant was collected and used for the stability study. 100 μl (~29.6MBq/0.8mCi) of ^{99m}Tc -MTX was incubated with 900 μl of plasma at 37°C. At 2 and 4 h, 100- μl aliquots were treated with a two-fold excess of ethanol and centrifuged at 1,000 x g for 15 min. The remaining pellet was washed thrice with 1 ml EtOH, and these ethanolic washes were combined with the supernatant and counted in a γ well counter. This activity was compared to the activity in the pellet, to give the percentage of ^{99m}Tc -MTX not bound to proteins. The supernatant was analysed by paper chromatography and ITLC, as described above.

Determination of partition coefficient. The apparent partition coefficient for ^{99m}Tc -MTX was determined by mixing aliquots of the technetium complex with 1-octanol and phosphate buffer (0.125 M, pH 7.4).

In a centrifuge tube, containing 2 ml of each phase, 100 μl of the ^{99m}Tc complex solution was added, and the mixture was agitated on a Vortex mixer for approximately 1 min and finally centrifuged at 5,000 x g for 5 min. Three samples (0.2 ml each) from each layer were counted in a γ counter. The partition coefficient was calculated as the mean value of each cpm/ml of octanol layer divided by that of the buffer. A sample (1.0 ml) from the octanol layer was subsequently repartitioned in octanol/buffer until constant values were obtained. This was achieved with the third repartition.

Biodistribution studies. All applicable institutional and/or national guidelines for the care and use of animals were followed. These studies were approved by the Ethics Committee of the National Center for Scientific Research of 'Demokritos' (Athens, Greece) and animal care and procedures followed are in accordance with institutional guidelines and licenses issued by the Department of Agriculture and Veterinary Policies of the Prefecture of Attiki (Registration nos. EL 25 BIO 022 and EL 25 BIO 021). Mice were housed under constant environmental conditions with 12 h light-dark cycles and had free access to food and water. To induce inflammation, animals were inoculated with 50 μl of pure turpentine oil subcutaneously in the left thigh muscle under slight ether anaesthesia (11,12). All animals developed an oedema 18 to 24 h after turpentine inoculation, which was visible to the naked eye.

Ex vivo animal experiments were performed in Swiss Albino mice with experimentally-induced inflammation (20 \pm 2 g, n=3 animals per time-point), by injecting 100 μl (3.7 MBq/0.1 mCi)

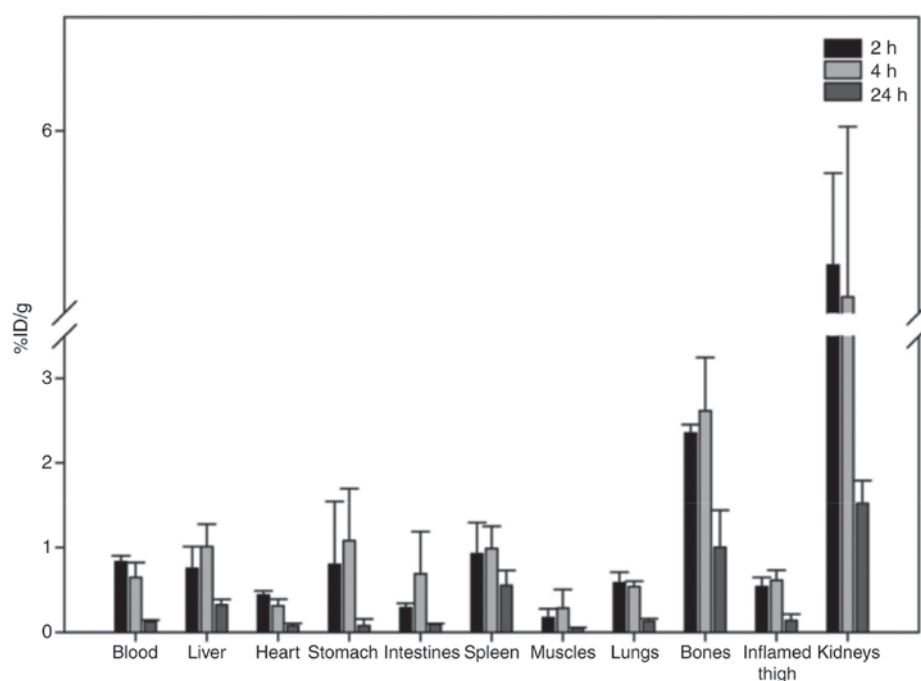


Figure 1. *Ex vivo* biodistribution of ^{99m}Tc -methotrexate in Swiss Albino mice, at 2, 4 and 24 h post injection (n=3 mice per time-point).

of the radiotracer via the tail vein. Animals were sacrificed by cardiectomy under slight ether anaesthesia at 2, 4 and 24 h post injection, and the main tissues and organs (blood, heart, liver, stomach, intestines, spleen, lungs, pancreas and bones) were excised, blotted dry and weighed. The inflamed thigh was excised and trimmed of the neighboring subcutaneous tissue. The muscle of the non-inflamed right thigh was also excised, for reasons of comparison. Samples were counted in a gamma counter (NaI gamma counter; Packard, Downers Grove, IL, USA). Standards were prepared from the injected material and were counted each time simultaneously with the tissues excised, allowing for calculations to be corrected for physical decay of the radioisotope. Radiolabeled MTX distribution over time was expressed as injected dose per gram (%ID/g).

Imaging system. The imaging system employed is a compact, Anger-type, γ -ray camera developed at the Center for Gamma-Ray Imaging of the University of Arizona. Details of the system can be found elsewhere (13-15). Briefly, the system comprises a 5 mm thick NaI(Tl) scintillation crystal, a 12 mm thick quartz light guide, a 3x3 array of 1.5 inch diameter photomultiplier tubes (PMTs), and a 40-mm thick lead parallel-hole collimator with hexagonal holes of 1-mm in diameter. The system achieves a spatial resolution of approximately 2.5 mm at the collimator face and degrades linearly with distance. The field-of-view of the camera is 4.5 in x 4.5 in, enough to image a whole mouse without axially moving the camera or the mouse.

Image acquisition. A Swiss mouse, with experimentally-induced inflammation for 24 h in the left hind limb area, was anesthetized with an intraperitoneal (IP) injection of ketamine (75 mg/kg) and xylazine (5 mg/kg) and placed on the camera face in the prone position. The animal was injected with 100 μl (25.9 MBq/0.7 μCi) of ^{99m}Tc -MTX. Dynamic planar

scintigraphy was performed by collecting 10 consecutive two-minute images, for a total period of 20 min. Two h after tracer injection, additional anaesthesia was applied and a 5-min static image was collected with the animal in the same position. Furthermore, 24 h after injection the animal was euthanized and a 1 h image was acquired.

Binding studies on hydroxyapatite. Hydroxyapatite binding studies were performed *in vitro* to simulate the binding of the radiotracer under investigation to bone structure. For this purpose, hydroxyapatite (Hap; Sigma-Aldrich; Merck KGaA, Darmstadt, Germany) was suspended in isotonic saline at 20 mg/ml and then incubated for 24 h at room temperature. The following day, 50 μl (0.444MBq/0.012mCi) of ^{99m}Tc -MTX were added to the Hap fractions. After a 10s vortex, the sample was incubated, under agitation, for 10 min at room temperature and centrifuged. The supernatant was then removed and the Hap fraction was washed twice with saline. The radioactivity of the Hap fraction and the saline washes were then measured with a well-type gamma counter. Control experiments were performed using ^{99m}Tc -MTX, without Hap. ^{99m}Tc -MTX binding to Hap was determined as percent of absorbed onto Hap [Hydroxyapatite binding (%)=(radioactivity of Hap fraction of each sample/total radioactivity)x100].

Results

Radiolabeling and radiochemical purity analysis. Radiolabeling of MTX was achieved by the preconjugation approach, via the precursor ^{99m}Tc -gluconate. Radiochemical purity was assessed by paper chromatography (Whatman 3 MM) and ITLC-SG. With ITLC-SG, ^{99m}Tc -MTX and the free pertechnetate $^{99m}\text{TcO}_4$ -appeared at $R_f=0.9-1.0$, while $^{99m}\text{TcO}_2$ was detected at $R_f=0.0-0.1$. In acetone the free $^{99m}\text{TcO}_4$ had an R_f of 0.9-1.0 while the ^{99m}Tc -MTX and the

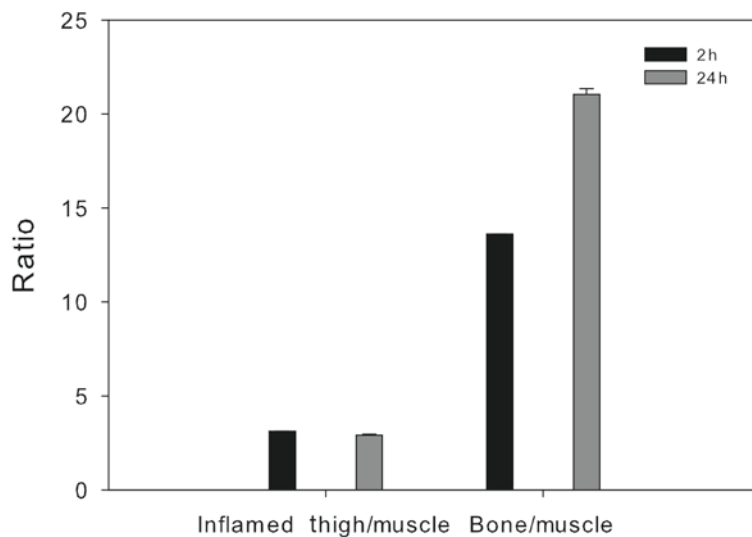


Figure 2. Inflammation-to-Muscle and Bone-to-Muscle ratios of ^{99m}Tc-methotrexate at 2 and 24 h post injection.

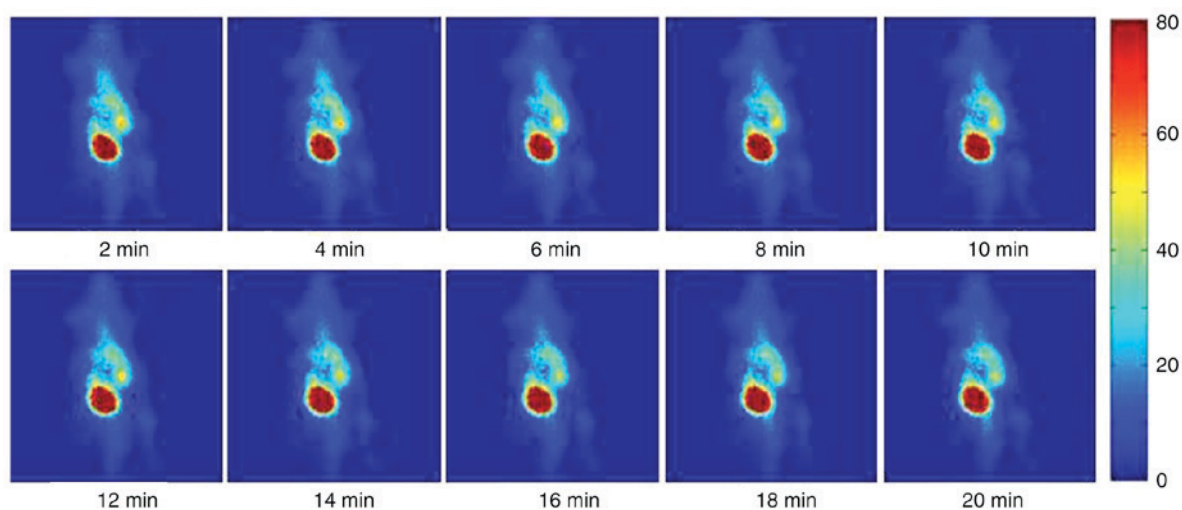


Figure 3. A dynamic sequence of 2-min γ -ray images of an inflammation-induced mouse injected with 0.7 mCi of ^{99m}Tc-methotrexate. All images are displayed using the same colour scale. The colour intensity represents the magnitude of the deposited radiotracer. The image acquisition began immediately following tracer injection. The bright red area on the left side of each picture corresponds to the inflammation site. Liver uptake was also observed.

hydrolysed ^{99m}TcO₂ appeared at Rf=0.0-0.1. The radiochemical purity of ^{99m}Tc-MTX was found to be 95-98%. Under the specific HPLC conditions, there was one product peak of ^{99m}Tc-MTX moving with the solvent front, with a retention time of approximately 20 min, while the retention times of ^{99m}TcO₄⁻ and ^{99m}Tc-gluconate were <5 min (9).

In vitro stability and protein binding. The stability of ^{99m}Tc-MTX was determined by paper chromatography and ITLC at different time points, as described above. The radiolabeled complex remained stable (up to 90%) at room temperature, for up to 24 h post-labelling. Plasma stability studies showed that 94.9±1.2% of ^{99m}Tc-MTX remained intact at 2 h, dropping to 85.8±2.7% at 4 h post-incubation.

Before performing *ex vivo* biodistribution studies in mice, the *in vitro* binding of ^{99m}Tc-MTX was assessed in

human plasma. Protein binding in human plasma was found to be 48.1±1.9% at 2 h, remaining practically stable at 4 h post-incubation (49.1±2.2%).

Determination of partition coefficient. Regarding lipophilicity, the partition coefficient indicated that ^{99m}Tc-MTX had maximum extraction in phosphate-buffered saline (PBS), pH 7.4 (hydrophilic medium), while a negligible amount of activity was observed in octanol (lipophilic medium), thus suggesting that radiolabeled drug was hydrophilic in nature. The logP value was estimated to be -2.28±0.03.

Biodistribution studies. The biodistribution of ^{99m}Tc-MTX was assessed on Swiss Albino mice with experimentally-induced inflammation at 2 and 24 h post injection (Fig. 1). Rapid clearance from blood and predominant excretion via the urinary

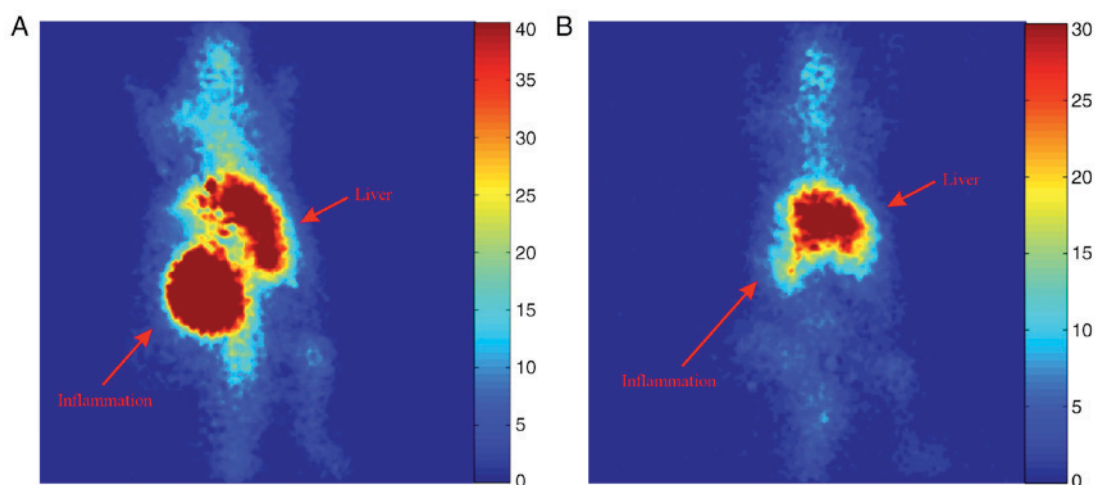


Figure 4. γ -ray scintigraphy of an inflammation-induced mouse injected with 0.7 mCi of ^{99m}Tc -methotrexate. (A) 5-min acquisition at 2 h post injection, and (B) 3 h acquisition at 24 h post injection. Increased uptake of the tracer can be visually identified in the site of inflammation as well as the liver at 2 h post injection. At 24 h post injection the majority of the tracer remains in the liver; however, some uptake at the joints and spine was also observed.

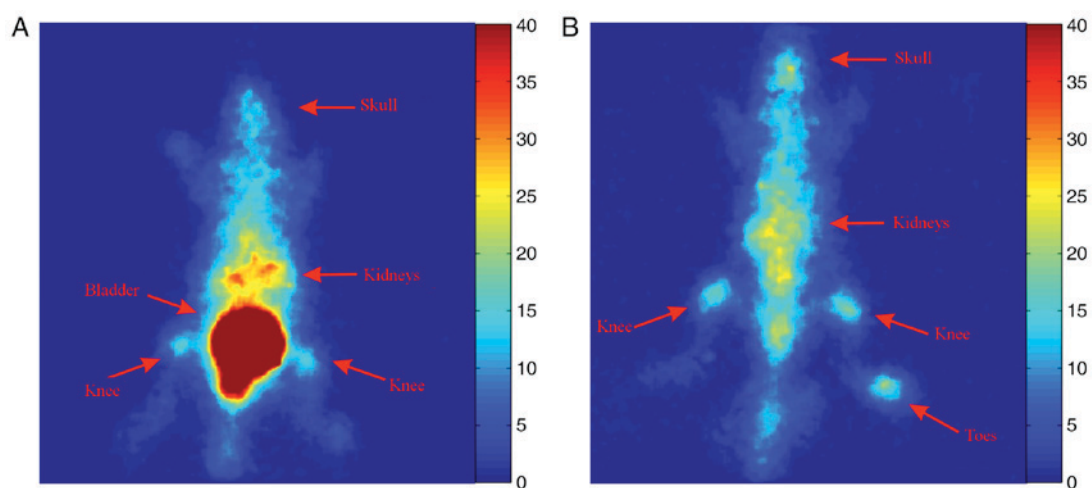


Figure 5. γ -ray scintigraphy of a mouse injected with 0.7 mCi of ^{99m}Tc -methotrexate. (A) 5-min acquisition at 2 h post injection, and (B) 1 h acquisition at 24 h post injection. Increased uptake of the tracer can be visually identified in the knees of the hind-limbs 2 h post injection. In addition, increased uptake is easily identified along the spine, in the hind-limb knees and the toes of the right hind-limb at 24 h post injection.

system was observed for the radiotracer. Uptake in the stomach and spleen was low, providing evidence for the *in vivo* stability of the tracer. With regard to the other organs, apart from the kidneys, no major uptake was observed in all analysed tissues ($\leq 1.0\%$ ID/g from 2 h post injection). An important observation was the increased uptake of the radiotracer in the inflamed muscle, in comparison to the contralateral normal muscle tissue (0.54 ± 0.11 vs. 0.17 ± 0.10 ; 0.61 ± 0.12 vs. 0.28 ± 0.22 ; and 0.14 ± 0.07 vs. 0.05 ± 0.01 at 2, 4 and 24 h post injection, respectively), with the inflammation-to-normal muscle ratio remaining practically stable up to 24 h post injection. Furthermore, an unexpected observation was the significant bone uptake observed, which led to a pronounced differentiation between bone and non-osseous tissue, especially at 24 h post injection (Fig. 2).

Imaging studies. A dynamic sequence of γ -ray images of an inflammation-induced mouse injected with 25.9 MBq (0.7 mCi) of ^{99m}Tc -MTX at consecutive time points is

presented in Fig. 3. All images are 2-min acquisitions and they are displayed on the same colour scale. The colour intensity represents the magnitude of the deposited radiotracer. The inflammation site, in the left side of the animal, is clearly identified by visual inspection immediately after injection. Liver uptake of the tracer is also observed at a lower concentration than the inflammation site.

Static planar scintigraphic images of the mouse at 2 and 24 h post injection are shown in Fig. 4. Increased uptake of the tracer can be visually identified in the inflammation site as well as the liver 2 h post injection. At 24 h post injection most of the tracer remains at the liver with very small uptake at the inflammation site. However, some uptake at the joints and spine is also observed both at 2 and 24 h after injection.

To assess the uptake of ^{99m}Tc -MTX at the bones and joints, a healthy mouse was injected with 0.7 mCi of ^{99m}Tc -MTX and planar images were acquired 2 and 24 h later. Increased uptake of the tracer was observed at the spine, the knees and the toes of the hind-limbs at both time points (Fig. 5).

Hydroxyapatite-binding assay. Hydroxyapatite binding of ^{99m}Tc -MTX was determined on a 20 mg/ml saline sample of Hap, and was found to be $44.9 \pm 1.3\%$, at 10 min post incubation. In the control experiments, we confirmed that the radioactivity adsorbed to the vials was less than 0.1%.

Discussion

MTX was first developed as a cancer treatment drug in the 1940, but won FDA approval for treating RA in the late 1980s. Since then, MTX has become the treatment of choice for people with this condition, as well as for other forms of inflammatory arthritis. In the present work, MTX radiolabeled with technetium-99m has been used to assess its capacity in imaging experimentally-induced inflammation in mice. Radiolabeling of MTX with Technetium-99m using gluconate as the transfer ligand gave comparable results to the work described by other groups (7,10), in terms of radiolabeling yield and stability of the radiolabeled product. With regard to the preparation of ^{99m}Tc , our method is much more facile and straightforward (10). Stability studies were performed to evaluate whether ^{99m}Tc -MTX is stable enough in plasma to ensure sufficient delivery of radioactivity to the site of interest, as only free (i.e., non-protein bound) radiotracer is available to diffuse out of the vasculature and localize in the organism. The stability of ^{99m}Tc -MTX was determined *in vitro* in human plasma, where it was shown that it remained intact up to 85% after 4 h. Plasma protein binding was found to be $48.1 \pm 1.9\%$ at 2 h, remaining practically stable at 4 h post-incubation ($49.1 \pm 2.2\%$).

The lipophilicity of ^{99m}Tc -MTX was determined by measuring its distribution between *n*-octanol and PBS, pH 7.4, and resulted in a logP value of -2.28 ± 0.03 , which is comparable to results of other groups. Indicatively we would like to refer to the work of Okarvi *et al* (10), who showed logP values of -2.01 and -1.90 , demonstrating a low lipophilicity of their ^{99m}Tc -MTX compounds. Our results showed that ^{99m}Tc -MTX is hydrophilic in nature, thus rapidly reaching the target area and exhibiting satisfactory clearance characteristics.

Biodistribution studies showed fast blood clearance, low hepatobiliary uptake and excretion via the urinary tract. The inflamed thigh showed higher radiotracer accumulation than the contralateral normal tissue, with an inflammation/muscle ratio of 3.12 ± 0.003 at 2 h post injection, slightly dropping to 2.92 ± 0.05 at 24 h post injection.

Planar imaging concurred with our biodistribution studies, with increased uptake at the inflammation area. However, increased uptake was also observed in the joints and spine, both areas with a relatively high remodelling activity. This prompted us to perform hydroxyapatite binding studies and a new planar scintigraphic study on a healthy mouse (without inflammation) after this pronounced uptake of ^{99m}Tc -MTX in the bone. The hydroxyapatite binding studies showed 45% binding of the tracer to the synthetic material, thus confirming the results of our biodistribution studies. Furthermore, the imaging study confirmed increased uptake of ^{99m}Tc -MTX in the spine and knee joints both at 2 and 24 h after injection (Fig. 5). These results combined with scintigraphic imaging results in the literature (16) might support the hypothesis that MTX has a diphosphonate-like behavior at least in the first 24 h, but further experiments are needed for clarification of these findings.

The interesting findings of our study have prompted us to further investigate ^{99m}Tc -MTX as a radiotracer for RA, as well as to demonstrate the efficacy of MTX before it is prescribed as a therapeutic agent for RA. If RA lesions accumulate radio-labeled MTX, these patients could be candidates for MTX therapy, while if the lesions are not addressed, the physician may proceed to the next line of treatment, without delays due to ineffective treatment. It is clear that a test which could predict adequate candidates for MTX treatment and response to MTX therapy would be welcomed by the rheumatology community. This might be of greater interest now that RA has been recognized as a major adverse event of immune checkpoint-inhibitor treatments for cancer (17).

MTX has been successfully labelled with ^{99m}Tc , with a radiochemical purity of $>95\%$. Stability was assessed in plasma, where it remained intact up to 85% at 4 h post-incubation. Preclinical *ex vivo* biodistribution studies as well as *in vivo* imaging studies have shown that ^{99m}Tc -MTX accumulates in inflammatory sites, as well as in the spine, the joints and bones, areas with relatively high remodelling activity.

To the best of our knowledge, this study is the first to report direct evidence of hydroxyapatite binding of ^{99m}Tc -MTX. This information might prove useful in the current research for bone-targeted drug delivery (18,19). The results are promising and set the stage for further study on the development and application of ^{99m}Tc -MTX as a tool for early detection and imaging of inflammation in RA.

Acknowledgements

The publication of this article was funded by the Onassis Scholars' Association of the 'Alexander S. Onassis' Public Benefit Foundation. Dr L. Furenlid was partially supported by The National Institutes of Health/National Institute of Biomedical Imaging and Bioengineering (grant no. P41-EB002035).

References

1. Rang HP, Dale MM, Ritter JM, Flower RH and Henderson G: Anticancer drugs. In: Pharmacology. 7th edition. Rang HP and Dale MM (eds). Churchill Livingstone Elsevier, London, 673-688, 2011.
2. Weinblatt ME: Methotrexate in rheumatoid arthritis: A quarter century of development. *Trans Am Clin Climatol Assoc* 124: 16-25, 2013.
3. Chan ES and Cronstein BN: Mechanisms of action of methotrexate. *Bull Hosp Jt Dis* 71 (Suppl 1): S5-S8, 2013.
4. Cutolo M, Sulli A, Pizzorni C, Serio B and Straub RH: Anti-inflammatory mechanisms of methotrexate in rheumatoid arthritis. *Ann Rheum Dis* 60: 729-735, 2001.
5. Tian H and Cronstein BN: Understanding the mechanisms of action of methotrexate: Implications for the treatment of rheumatoid arthritis. *Bull NYU Hosp Jt Dis* 65: 168-173, 2007.
6. Wessels JA, Huizinga TW and Guchelaar HJ: Recent insights in the pharmacological actions of methotrexate in the treatment of rheumatoid arthritis. *Rheumatology (Oxford)* 47: 249-255, 2008.
7. Dar UK, Khan IU, Javed M, Ahmad F, Ali M and Hyder SW: Preparation and biodistribution in mice of a new radiopharmaceutical-technetium-99m labeled methotrexate, as a tumor diagnostic agent. *Hell J Nucl Med* 15: 120-124, 2012.
8. Rasheed R, Javed M, Ahmad F, Sohail A, Murad S, Masood M, Rasheed S and Rasheed S: Preparation of (^{99m}Tc)-labelled methotrexate by a direct labeling technique as a potential diagnostic agent for breast cancer and preliminary clinical results. *Hell J Nucl Med* 16: 33-37, 2013.

9. Ozgenc E, Ekinci M, Ilem-Ozdemir D, Gundoglu E and Asikoglu M: Radiolabeling and in vitro evaluation of ^{99m}Tc -methotrexate on breast cancer cell line. *J Radioanal Nucl Chem* 307: 627-633, 2016.
10. Okarvi SM and Jammaz IA: Preparation and in vitro and in vivo evaluation of technetium-99m-labeled folate and methotrexate conjugates as tumor imaging agents. *Cancer Biother Radiopharm* 21: 49-60, 2006.
11. Mirzaei A, Jalilian AR, Akhlaghi M and Beiki D: Production of ^{68}Ga -citrate based on a SnO_2 generator for short-term turpentine oil-induced inflammation imaging in rats. *Curr Radiopharm* 9: 208-214, 2016.
12. Rivera S and Ganz T: Animal models of anemia of inflammation. *Semin Hematol* 46: 351-357, 2009.
13. Furenlid LR, Wilson DW, Chen YC, Kim H, Pietraski PJ, Crawford MJ and Barrett HH: FastSPECT II: A second-generation high-resolution dynamic SPECT imager. *IEEE Trans Nucl Sci* 51: 631-635, 2004.
14. Furenlid LR, Chen YC and Kim H: SPECT Imager Design and Data-Acquisition Systems. In: *Small-Animal SPECT Imaging*. Kupinski MA and Barrett HH (eds). Springer US, Boston, MA, pp115S-138S, 2005.
15. Chen YC, Furenlid LR, Wilson DW and Barrett HH: Calibration of Scintillation Cameras and Pinhole SPECT Imaging Systems. In: *Small-Animal SPECT Imaging*. Kupinski MA and Barrett HH (eds) Springer US, Boston, MA, 195-201, 2005.
16. Rasheed R, Gillani J, Jielani A, Irum F, Lodhi N, Rasheed S and Rasheed S: Tc^{99m} methotrexate (MTX): A novel complex for imaging of rheumatoid arthritis (RA): First clinical trials. *Gen Med (Los Angel) Personalized Medicine*: S213, 2016.
17. Naidoo J, Cappelli LC, Forde PM, Marrone KA, Lipson EJ, Hammers HJ, Sharfman WH, Le DT, Baer AN, Shah AA, *et al*: Inflammatory arthritis: A newly recognized adverse event of immune checkpoint blockade. *Oncologist* 22: 627-630, 2017.
18. Cole LE, Vargo-Gogola T and Roeder RK: Targeted delivery to bone and mineral deposits using bisphosphonate ligands. *Adv Drug Deliv Rev* 99: 12-27, 2016.
19. Raichur V, Vemula KD, Bhadri N and Razdan R: Zolendronic acid-conjugated PLGA ultrasmall nanoparticle loaded with methotrexate as a supercarrier for bone-targeted drug delivery. *AAPS PharmSciTech* 18: 2227-2239, 2017.